Hydrate phase transition and seepage mechanism during natural gas hydrates production tests in the South China Sea: A review and prospect

Xu–wen Qin, Cheng Lu, Ping–kang Wang, Qian–yong Liang

Citation: Xu–wen Qin, Cheng Lu, Ping–kang Wang, Qian–yong Liang, 2022. Hydrate phase transition and seepage mechanism during natural gas hydrates production tests in the South China Sea: A review and prospect, China Geology, 5, 201–217. doi: 10.31035/cg2022029.

View online: https://doi.org/10.31035/cg2022029

China Geology 5 (2022) 201−217

China Geology

Journal homepage: http://chinageology.cgs.cn
https://www.sciencedirect.com/journal/china-geology

Special Reviews

Hydrate phase transition and seepage mechanism during natural gas hydrates production tests in the South China Sea: A review and prospect

Xu-wen Qin[a, b, c], Cheng Lu[a, b, c, d], Ping-kang Wang[a], Qian-yong Liang[b, c]

[a] *China Geological Survey*, *Ministry of Natural Resources*, *Beijing* 100037, *China*
[b] *Guangzhou Marine Geological Survey*, *China Geological Survey*, *Ministry of Natural Resources*, *Guangzhou* 510075, *China*
[c] *Gas Hydrate Engineering Technology Center*, *China Geological Survey*, *Ministry of Natural Resources*, *Guangzhou* 510075, *China*
[d] *Oil and Gas Resources Survey*, *China Geological Survey*, *Ministry of Natural Resources*, *Beijing* 100083, *China*

A R T I C L E I N F O

Article history:
Received 29 January 2022
Received in revised form 17 March 2022
Accepted 15 April 2022
Available online 25 April 2022

Keywords:
Natural gas hydrates
Clayey silt reservoir
Hydrate phase transition
Seepage mechanism
Oil and gas exploration engineering
NGHs exploration trial engineering
South China Sea
China

A B S T R A C T

Natural gas hydrates (NGHs) are globally recognized as an important type of strategic alternative energy due to their high combustion efficiency, cleanness, and large amounts of resources. The NGHs reservoirs in the South China Sea (SCS) mainly consist of clayey silts. NGHs reservoirs of this type boast the largest distribution range and the highest percentage of resources among NGHs reservoirs in the world. However, they are more difficult to exploit than sandy reservoirs. The China Geological Survey successfully carried out two NGHs production tests in the Shenhu Area in the northern SCS in 2017 and 2020, setting multiple world records, such as the longest gas production time, the highest total gas production, and the highest average daily gas production, as well as achieving a series of innovative theoretical results. As suggested by the in-depth research on the two production tests, key factors that restrict the gas production efficiency of hydrate dissociation include reservoir structure characterization, hydrate phase transition, multiphase seepage and permeability enhancement, and the simulation and regulation of production capacity, among which the hydrate phase transition and seepage mechanism are crucial. Study results reveal that the hydrate phase transition in the SCS is characterized by low dissociation temperature, is prone to produce secondary hydrates in the reservoirs, and is a complex process under the combined effects of the seepage, stress, temperature, and chemical fields. The multiphase seepage is controlled by multiple factors such as the physical properties of unconsolidated reservoirs, the hydrate phase transition, and exploitation methods and is characterized by strong methane adsorption, abrupt changes in absolute permeability, and the weak flow capacity of gas. To ensure the long-term, stable, and efficient NGHs exploitation in the SCS, it is necessary to further enhance the reservoir seepage capacity and increase gas production through secondary reservoir stimulation based on initial reservoir stimulation. With the constant progress in the NGHs industrialization, great efforts should be made to tackle the difficulties, such as determining the micro-change in temperature and pressure, the response mechanisms of material-energy exchange, the methods for efficient NGHs dissociation, and the boundary conditions for the formation of secondary hydrates in the large-scale, long-term gas production.

1. Introduction

Natural gas hydrates (NGHs), which are usually called methane hydrates, refer to ice-like crystalline compounds formed from hydrocarbon gases (mainly methane) and water in stable areas under certain temperature and pressure conditions. More than 90% of NGHs occur in submarine sediments at shelf margins, and less than 10% are distributed in fractures and pores of rocks in continental permafrost. 1 m^3 of NGHs can be decomposed into 0.8 m^3 of water and approximately 164 m^3 of natural gas under standard temperature and pressure. Moreover, NGHs almost produce no residue after combustion and are thus a type of clean, abundant energy resource with high combustion (Li JF et al., 2018). It is estimated that the total global resources of natural gas contained in NGHs is approximately 2.1×10^{16} m^3 (Sloan ED et al., 2007). To promote the development and utilization

First author: *E-mail address*: qinxuwen@163.com (Xu-wen Qin).

Literary editor: Xi-jie Chen
doi:10.31035/cg2022029

of NGHs resources, Canada and the United States conducted three NGHs production tests using vertical wells in non-diagenetic glutenite and sandstone reservoirs in continental frozen soil areas, while Japan completed two production tests using vertical wells in offshore sandy reservoirs (Moridis GJ et al., 2005; Numasawa M et al., 2008; Schoderbek D et al., 2013; Hauge LP et al., 2014; Terao Y et al., 2014; Oyama A et al., 2017). However, none of these production tests achieved their expected gas production targets due to problems such as sand production and low gas-production efficiency (Table 1). The NGHs reservoirs in the SCS mainly consist of clayey silts. The NGHs reservoirs of this type are distributed the mostly widely across the world, with natural gas resources accounting for approximately 90% of the global resources. However, compared with the non-diagenetic glutenite and sandstone reservoirs and sandy reservoirs, the clayey silt reservoirs have extremely low porosity and permeability, making them extremely difficult to exploit. To meet these challenges, China has implemented innovative techniques and methods for NGHs production tests through theoretical research and simulation experiments. As a result, it successively made breakthroughs in the technologies for drilling and gas recovery using vertical wells and horizontal wells in deep-sea shallow and soft strata, and completed an exploratory and an experimental production test in the Shenhu Area in the SCS, respectively in 2017 and 2020 (Fig. 1; Li JF et al., 2018; Ye JL et al., 2020).

Overall, China has made considerable progress in NGHs exploration and exploitation. Specifically, it has developed a series of innovative understandings of the characteristics, formation and evolution, migration and accumulation, and production test techniques of NGHs through massive investigations and by tackling technological challenges (Li XS et al ., 2008; Zou CN et al., 2013; Wu NY et al., 2017; Li

Table 1. NGHs production tests in major countries.

Country	Area	Reservoir type	Year	Type of production wells and method	Duration /days	Cumulative gas production/ m^3
China	Shenhu Area, SCS	Clayey silts	2017	Vertical wells; depressurization	60	30.9×10^4
	Shenhu Area, SCS		2020	Horizontal wells; depressurization	42	149.86×10^4
Canada	Mackenzie Delta	Glutenites (non-diagenetic)	2002	Vertical wells; hot water circulation	5	516
	Mackenzie Delta		2007–2008	Vertical wells; depressurization	6	1.3×10^4
America	North Slope in Alaska	Sandstones (non-diagenetic)	2012	Vertical wells; CO_2 displacement + depressurization	30	2.4×10^4
Japan	Nankai Trough, Japan	Sandy sediments	2013	Vertical wells; depressurization	6	12×10^4
	Nankai Trough, Japan		2017	Vertical wells; depressurization	12	3.5×10^4
					24	20×10^4

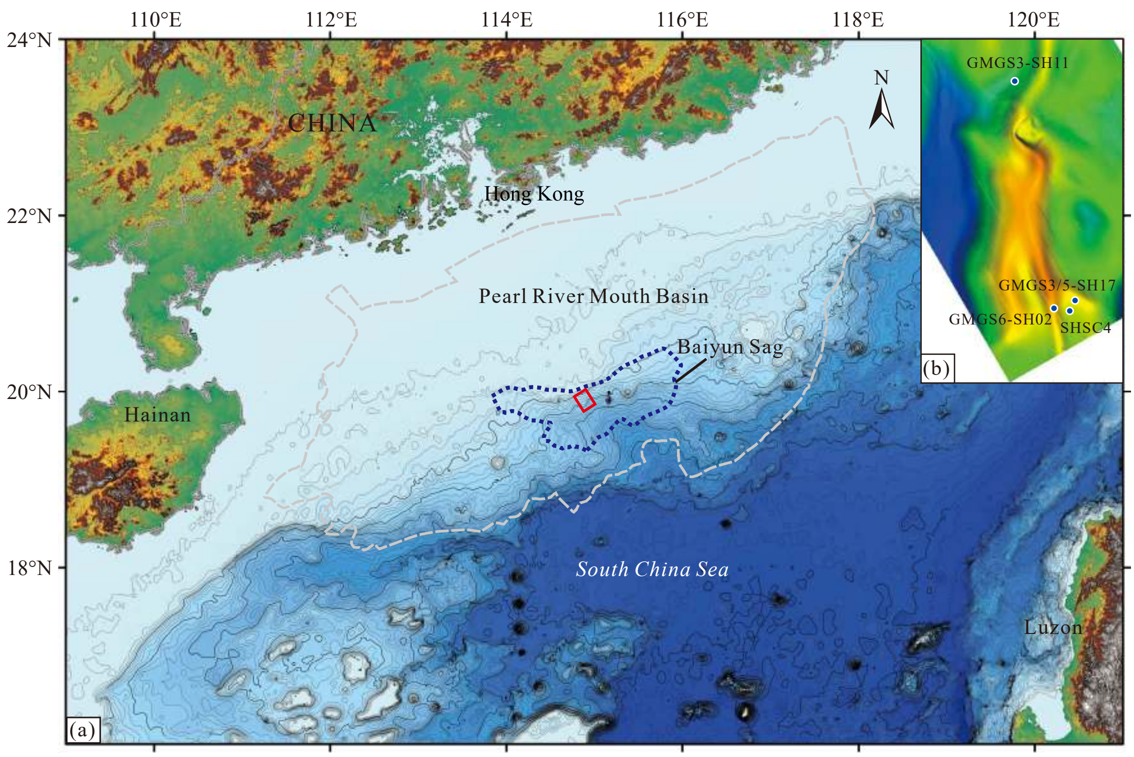

Fig. 1. Geological map of the study area; a–regional geological background and the location of the study area (marked with a red square); b–relative location of Well GMGS5-SH17 (after Qin XW et al., 2020).

JF et al., 2018; Ye JL et al., 2020; Qin XW et al., 2020; Yang CZ et al., 2020; Su PP et al., 2020; Zhang W et al., 2020; Zhong GF et al., 2020; Wei N et al., 2020; Ning FL et al., 2020; Gao DL, 2020; Wu NY et al., 2020; Sun JS et al., 2021). Previous studies on NGHs exploitation mechanisms mainly focused on the mechanical responses and physical changes of reservoirs, the simulation and prediction of the reservoir production capacity, and the R&D and application of reservoir simulators (Li SX et al., 2020; Wei CF et al., 2020; Cai JC et al., 2020; Lu HL et al., 2021; Wu NY et al., 2021). In recent years, the authors have carried out in-depth research on the two NGHs production tests in the Shenhu Area in the SCS and discovered that the key factors restricting the gas production efficiency reservoir structure characterization of, hydrate phase transition, multiphase seepage and permeability enhancement, and the simulation and regulation of production capacity, among which the hydrate phase transition and seepage mechanism are the most crucial (Qin XW et al., 2019a, 2019b, 2020; Lu C et al., 2019a; 2019b; Li SD et al., 2020; Cai JC et al., 2020; Bian H et al., 2020; Qi RR et al., 2021, 2022; Geng LT et al., 2021; Lu C et al., 2021a; 2021b; 2021c; Xu T et al., 2021; Lei X et al., 2022). This study systematically reviews and summarizes the progress in the research on the phase transition and seepage mechanism of hydrates in NGHs reservoirs in the SCS, aiming to reveal the dissociation mechanism, occurrence pattern, and production increase mechanism of hydrates and thus to provide the theoretical bases for the development and utilization of hydrate resources.

2. Physical properties of NGHs reservoirs in the SCS

2.1. Mineral composition and pores

The clayey silt reservoirs in the SCS contain large amounts of quartz and feldspar minerals with a poor roundness. Moreover, they bear many microbial fossils dominated by foraminifera. The clay minerals mainly consist of illites and mostly fill between quartz and feldspars. The pores in the reservoirs mainly include the pores of microbial fossils, intergranular pores, the intercrystalline pores of clay and mica, and dissolution pores, with pores of clay and microfossils dominating (Fig. 2). As shown by the whole-rock and clay mineral analyses, samples differ greatly in the content and distribution of minerals. Some samples consist of quartz primarily and clay secondarily, while some samples are dominated by carbonate rocks but have a low quartz content. However, the clay minerals in all types of NGHs reservoirs are dominated by illites, which compose more than 75% of total clay content (Fig. 3).

The average pore radii of the reservoirs in the SCS vary greatly. For instance, microbial fossils have large pore radii, while clay has small pore radii. The reservoirs have small median pore radii, all of which are less than 1.5 μm. In addition, there are large amounts of submicron pores, which mainly include interlayer pores of clay minerals, intragranular pores, intergranular pores, and large pores among clay particles (Lei X et al., 2022). Furthermore, pores with radii of less than 1 μm account for up to 75% in reservoirs dominated by carbonate rocks (Fig. 4 and Table 2).

Overall, the clayey silt reservoirs in the SCS have a high content of clay minerals. As a result, the water from hydrate dissociation will cause clay minerals to swell during NGHs exploitation, leading to blockage of pores and their throats. Therefore, the NGHs exploitation of the clayey silt reservoirs pose risks of decrease in the absolute and effective

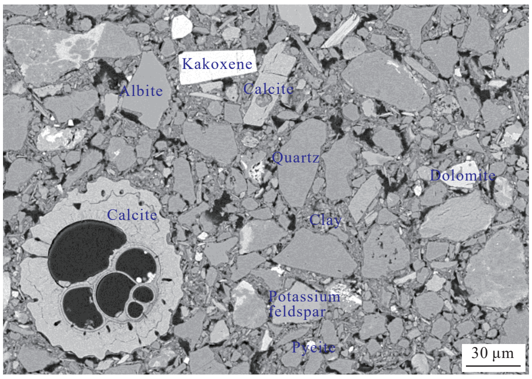

Fig. 2. Typical mineral surfaces of reservoir samples.

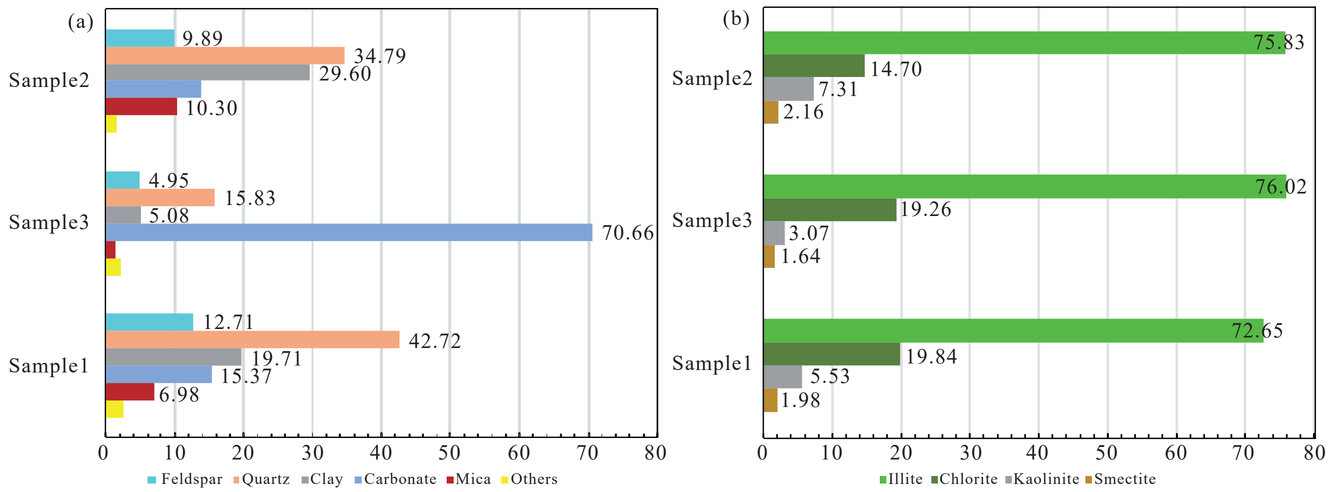

Fig. 3. Comparison of mineral and clay contents of three samples.

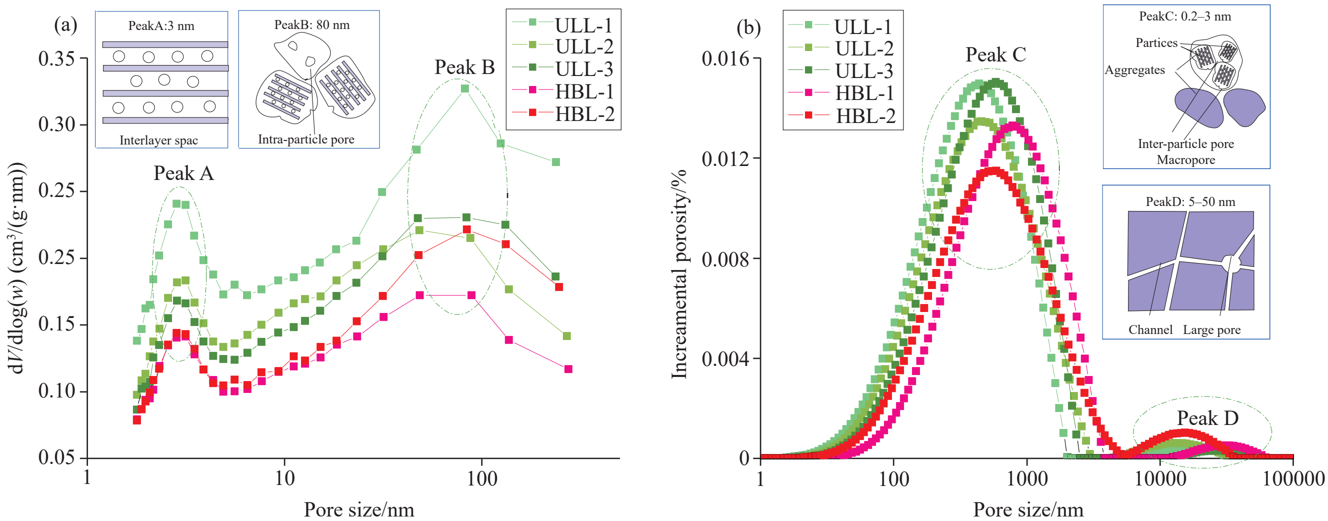

Fig. 4. Distribution of pore sizes and pore types based on (a) N2-adsorption and (b) NMR.

Table 2. Comparison of pore radius parameters between samples.

Sample	Porosity/ %	Average pore radius /μm	Median pore radius /μm	Submicron pore fraction/%
1	16.78	1.543	1.341	38.9
2	24.14	4.1	1.23	45
3	20.77	2.86	0.6	75

permeability of the reservoirs. Moreover, the high percentage of submicron pores result in ultra-low permeability, thus reducing the flow capacities of gas and water from hydrate dissociation and increasing the difficulty in NGHs exploitation.

2.2. Characterization of pore structure

Compared with diagenetic reservoirs, clayey silt reservoirs are loose and unconsolidated. Given that the three-dimensional structure of the porous media of reservoirs can be accurately obtained using computed tomography (CT) and digital core technology, the authors obtained the spatial distribution of reservoir pore structure through CT scanning of clayey silt reservoir samples and obtained the permeability of the samples through simulation. The results showed that the clayey silt reservoirs have significant high porosity and ultra-low permeability (Fig. 5).

The pore structure characterization and porosity-permeability correlations of clayey silts were determined as follows in this study. Firstly, the authors conducted a traditional Euclidean analysis and found that porosity did not correlate well with permeability and thus cannot be used to accurately characterize the pore structure complexity of clayey silts in the SCS (Fig. 6a). Afterward, taking advantage of the fractal geometry theory, which can quantify the complex spatial pore structure (Cai JC et al., 2015), the authors employed the fractal dimension and succolarity values to characterize the complex micropore structure of the clayey silt reservoirs. Compared with conventional sandstone reservoirs, clayey silt reservoirs have higher fractal dimensions under conditions of similar porosity. This finding further proves that clayey silt reservoirs have more complex spatial pore distribution than conventional sandstone reservoirs (Table 3). Moreover, there is a close correlation between the succolarity values and permeability of clayey silt reservoir samples (Fig. 6b; Bian H et al., 2020). Therefore, it is feasible to use the fractal geometry theory to build the permeability fitting model of the clayey silt reservoirs in the SCS, in order to conduct in-depth analyses of the law of the changes in reservoir permeability during the NGHs production tests in the SCS.

3. NGHs phase transition

3.1. Molecular dynamics study of NGHs

Over the past few years, the molecular dynamics study of hydrates has advanced constantly from gas mixtures and simple liquids to complex materials such as polymers and nanoparticles, revealing the nucleation and dissociation mechanism of hydrates (Khurana J et al., 2017; Kondori J et al., 2017; Teixeira AMA et al., 2018; Liu W et al., 2019). Based on the molecular dynamics analysis of hydrate samples taken from different types of reservoirs, the authors believe that it is necessary to further consider the effects of factors such as the crystallinity and hydrophilicity of the solid surface of reservoirs to establish a more practical solid molecular model in the study of the nucleation and dissociation mechanism of hydrates in the SCS. Moreover, a study has suggested that the kinetic inhibitors, such as pectin, chitosan, cassava powder, and antifreeze protein, can effectively inhibit the nucleation or the crystal growth of hydrates, thus reducing the formation of secondary hydrates in reservoirs and the production well shaft plugging during NGHs exploitation (Fig. 7; Qi RR et al., 2021). Determining the functional mechanism of inhibitors and screening economical and efficient kinetic inhibitor materials are still long-term research topics.

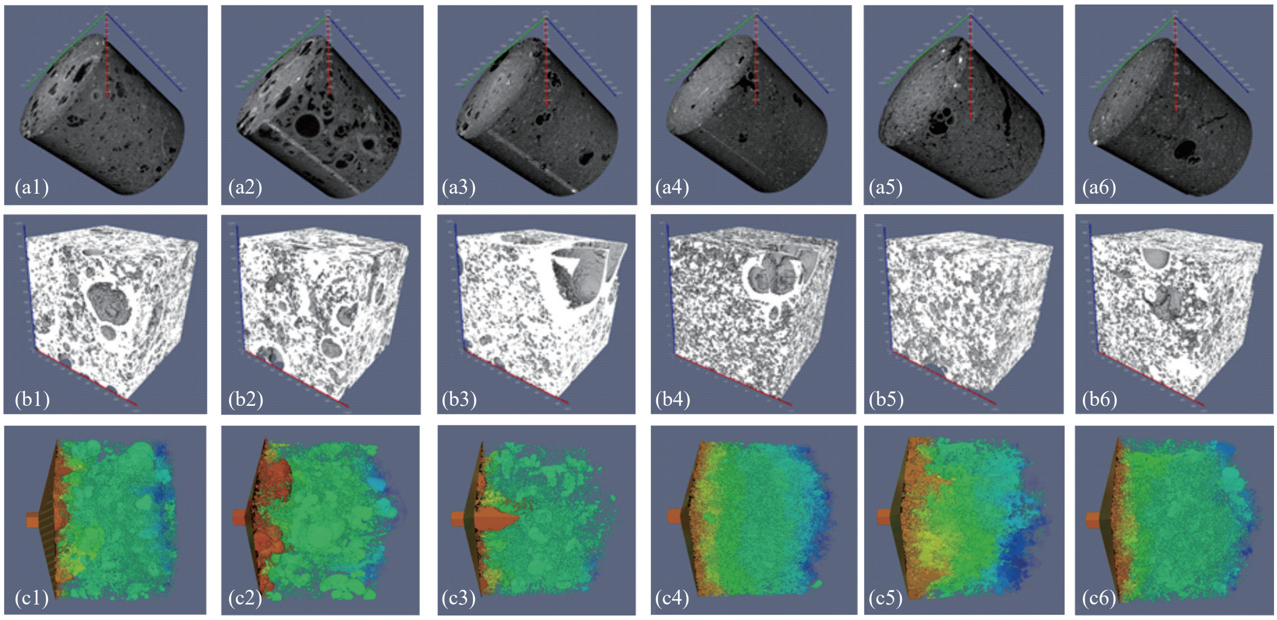

Fig. 5. Original grayscale images (a) and binarized images (b, 5123 pixels) of six hydrate reservoir samples, and the pressure field (Pa) distributed along *y* direction in the permeability simulation of six hydrate samples (c). In the binarized images, the gray and white portions denote pores and solid, respectively (after Bian H et al., 2020).

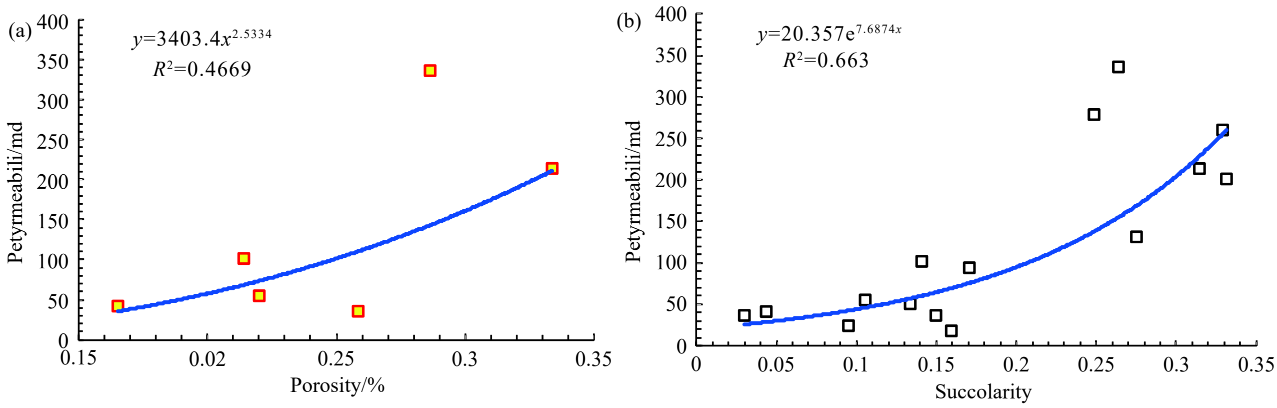

Fig. 6. Schematic diagram of porosity and permeability fitting of six hydrate samples (a); fitted curve of succolarity and permeability for six hydrate samples along different positive directions (b) (after Bian H et al., 2020).

Table 3. Calculated 3D fractal dimensions of six hydrate samples and two sandstone cores (after Bian H et al., 2020).

Parameter	Sample 1	Sample 2	Sample 3	Sample 4	Sample 5	Sample 6	Core a	Core b
Fractal dimension	2.77	2.79	2.71	2.85	2.81	2.78	2.70	2.85

3.2. Hydrate phase equilibrium

Understanding hydrate phase equilibrium conditions and obtaining accurate parameters of hydrate phase equilibrium curves are the basis for revealing the complex hydrate phase transition and seepage laws, regulating production capacity, and developing depressurization strategies of reservoirs in the SCS. Previous studies on the hydrate phase equilibrium of the SCS were carried out using pure CH_4 gas rather than the methane gas released from hydrate dissociation, or NaCl solution instead of seawater, or artificially prepared single/mixed media rather than sediment reservoirs (Lu H et al., 2002; Uchida T et al., 2004; Sun SC et al., 2015; Zhang Y et al., 2016; Lü Q et al., 2018; Wang XH et al., 2019; Mu L et al., 2019).

Based on the reservoir samples collected from the NGHs production test area in the Shenhu Area, the authors prepared the gas and water sources required for the phase equilibrium experiments using the *in situ* salt ion content in pore water and gas composition. Then, using the gradient heating method and the improved Chen-Guo model, the hydrate phase equilibrium conditions of the SCS were obtained from the system containing salt ions and porous sediments (Geng LT et al., 2021). Compared with pure methane hydrates, the hydrate phase equilibrium curves of clayey silts in the SCS significantly shifted to the left and showed much lower hydrate dissociation temperature. This phenomenon occurred due to the hydrophily of the porous media and the capillary force produced by large numbers of submicron pores in clayey silts, which reduce water activity. Moreover, the hydrate phase equilibrium curves gradually moved toward the low-temperature high-pressure zone with an increase in the salinity. The improved Chen-Guo model has high precision, with an average deviation of only 3.7% in predicting the average pressure of sediments, thus greatly improving the accuracy of the production capacity simulation of hydrate production tests (Fig. 8). Moreover, the hydrates in the clayey silts in the SCS showed significantly increased dissociation enthalpy and tended to be more stable with a decrease in salinity. These results indicate that the depressurization-induced dissociation of hydrates in clayey silts will lead to an increasingly significant drop in reservoir temperature and make secondary hydrates more likely to form in reservoirs (Fig. 9).

3.3. Effects of hydrate phase transition on reservoir permeability

The porous media in clayey silts, which have complex mineralogical compositions and heterogeneous pore structures, have composite effects on hydrate phase transition. Moreover, hydrate phase transition will then cause changes in the reservoir physical properties such as porosity and permeability and thus affect gas production. Previous study results of the effects of hydrate phase transition on reservoir permeability were mostly obtained based on media such as artificial quartz sand or glass beads, while the actual reservoir conditions in the SCS have not been studied (Liu W et al.,

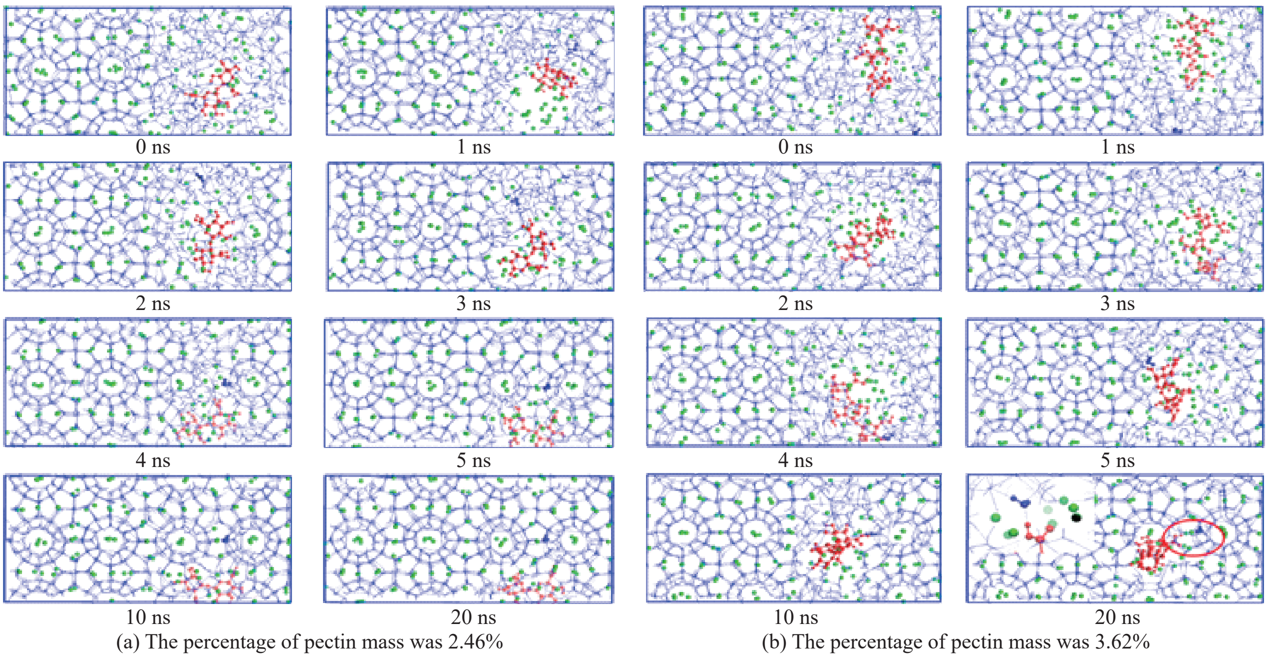

Fig. 7. Configurations of pectin at 0 ns, 1 ns, 2 ns, 3 ns, 4 ns, 5 ns, 10 ns, and 20 ns. Blue represents water molecules, blue dotted lines represent hydrogen bonds, green represents methane, and red represents pectin (after Qi RG et al., 2021).

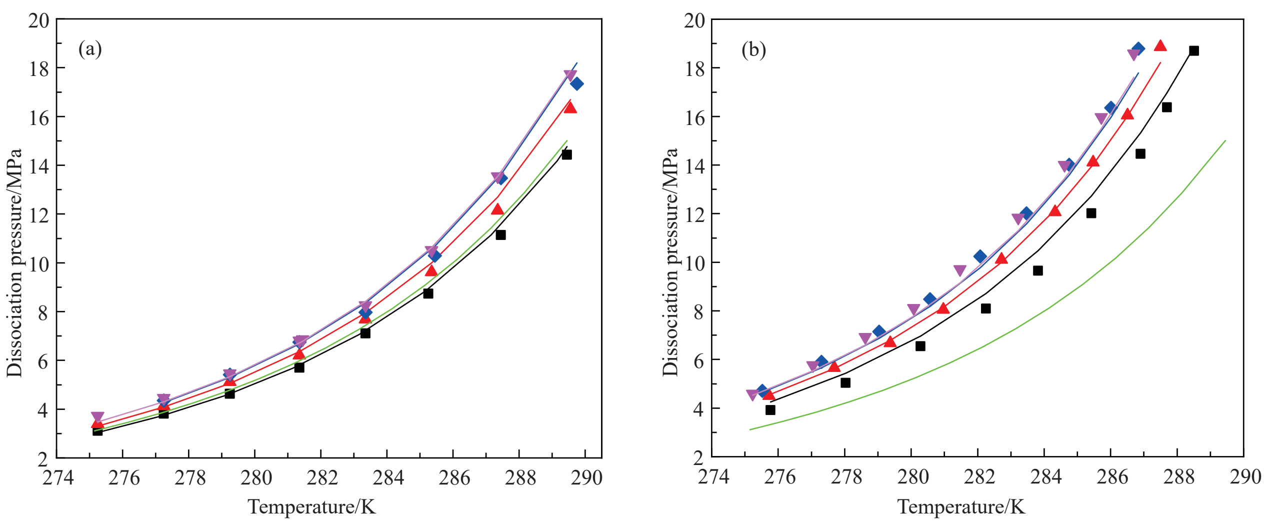

Fig. 8. NGHs dissociation conditions in bulk water (a) and in sediments (b) with different salinities: (■) deionized water, (▲) 1.97 wt%, (♦) 3.19 wt%, and (▼) 3.35 wt%, and corresponding calculated pressure denoted by solid lines calculated using the improved Chen-Guo. The green lines denote CH_4 hydrated in pure water calculated using the Chen-Guo model (after Geng LT et al., 2021).

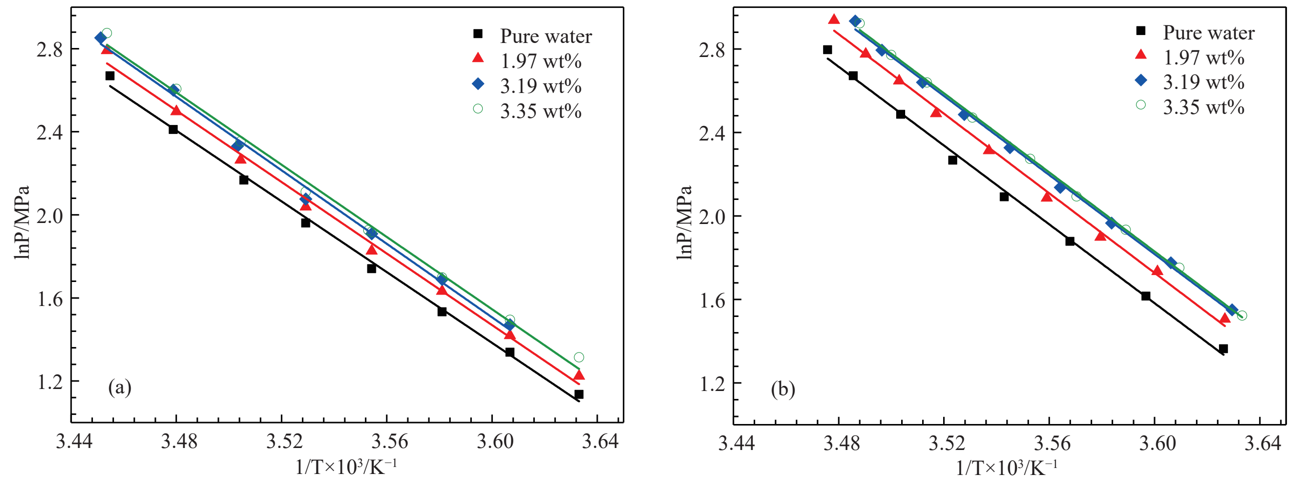

Fig. 9. The plots of reciprocal temperature (1/T) *vs.* the natural logarithm of dissociation pressure (lnP) for experimental NGHs in (a) the bulk water and (b) marine sediments. The solid lines indicate the reliability and accuracy of the experimental procedure and data points (after Geng LT et al., 2021).

2015; Kumar SW et al., 2015; Heeschen KU et al., 2016; Wang P et al., 2017; Zhang L et al., 2019; Song G et al., 2020; Li Z et al., 2020; Qin Y et al., 2021).

Based on the hydrate-dissociated clayey silt samples collected from the Shenhu Area, the authors studied the dynamic change in reservoir permeability with the evolution of hydrate phase transition using low-temperature and low-field nuclear magnetic resonance (LF-NMR) displacement devices. The results show that, similar to other types of hydrates, the hydrates in the porous media in clayey silts in the SCS change the pore structure of reservoirs, affect the flow of mobile fluids in the media, and induce the order of amplitude of the reservoir permeability to dynamically change. Presently, different permeability models established based on a single hydrate growth pattern or assumed conditions yield quite different fitting results. Therefore, they cannot precisely describe the dynamic relationship between hydrate saturation and the permeability of complex media in the process of the hydrate phase transition in clayey silts (Fig. 10). Therefore, the dynamic evolution of reservoir permeability during the hydrate exploitation from clayey silts is a complex process controlled by multiple mechanisms and factors.

3.4. Main factors controlling secondary hydrate formation

As shown by previous small-scale physical simulation experiments or numerical simulations (Yu M et al., 2017; Yamamoto K et al., 2017; Fan Z et al., 2017; Yu L et al., 2018; Chen L et al., 2018; Yang L et al., 2021; Li SX et al., 2021), the challenge that secondary hydrates and ice form at a low temperature during NGHs exploitation by depressurization must be tackled. Specifically, due to the combined effects of hydrate dissociation enthalpy and the Joule-Thomson effect, the local reservoir temperature will decrease to the hydrate phase equilibrium zone during the NGHs exploitation by depressurization. As a result, gas-water two-phase fluids occurring in porous media will form hydrates or ice again in a low-temperature and high-pressure environment, thus blocking the seepage channels and reducing the reservoir permeability. Consequently, the reservoir temperature and pressure will be redistributed, thus further affecting the hydrate dissociation and finally leading to a decrease in gas production. To further determine the main factors controlling the formation of secondary hydrates or ice in the actual NGHs exploitation environment, the authors, using the device for simulating the formation and evolution of NGHs inverse phase transition (Lu C et al., 2021), preliminarily analyzed the formation position and scale of secondary hydrates from the dissociation front to the production well shaft and investigated the effects of NGHs production-induced pressure difference on the formation of secondary hydrates.

This study shows that the reservoir temperature and pressure changed as follows under the same production-induced pressure difference. The decreased amplitude of reservoir temperature increased in area closer to well shaft in the initial hydrate dissociation stage due to the Joule-Thomson effect of gas. Then, it significantly decreased as the NGHs dissociation zone constantly expanded. As a result, the reservoir temperature maintained above the freezing point and the reservoir pressure basically remained stable around the well. Moreover, the throttling and expansion effect of gas weakened as the dissociation front spread. Accordingly, the hydrate stability zone expansion significantly slowed down, and the risks of secondary hydrate formation also greatly decreased (Fig. 11). The reservoir temperature and pressure changed as follows under the same hydrate dissociation range. Compared with a small pressure difference, a large pressure difference caused the reservoir temperature around the well to decrease more significantly. As a result, the local reservoir temperature and pressure points shifted leftward to the hydrate stability zone in a short time, resulting in a high formation rate of secondary hydrates and thus a significant decline in the gas production rate. By contrast, a small pressure difference caused low-saturation secondary hydrates to form but had little effect on gas production (Fig. 12). Therefore, the production-induced pressure difference plays an important role in controlling the formation of secondary hydrates.

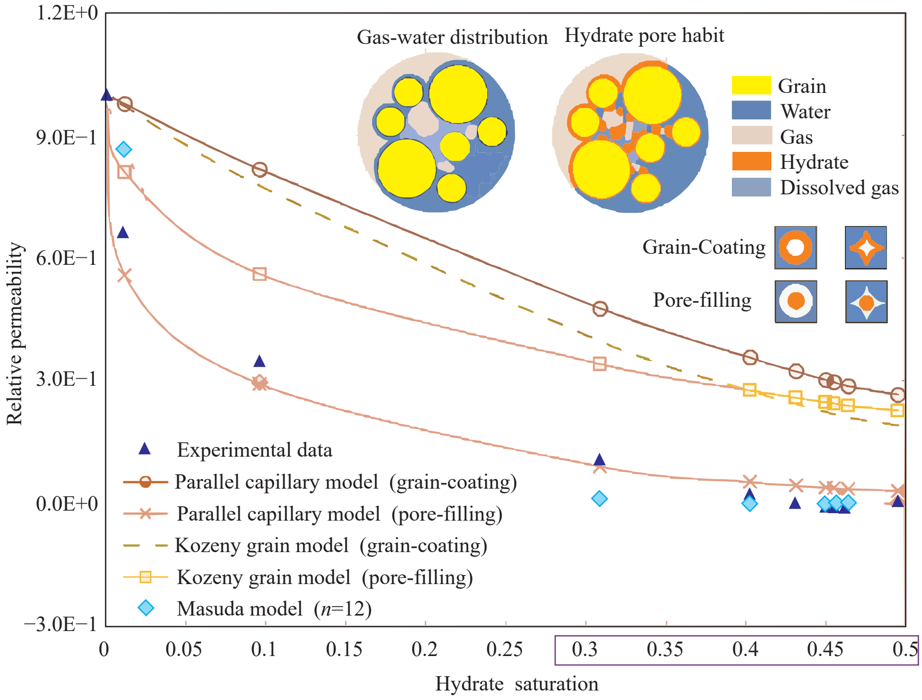

Fig. 10. Relationships between hydrate saturation and permeability/initial permeability calculated using various models.

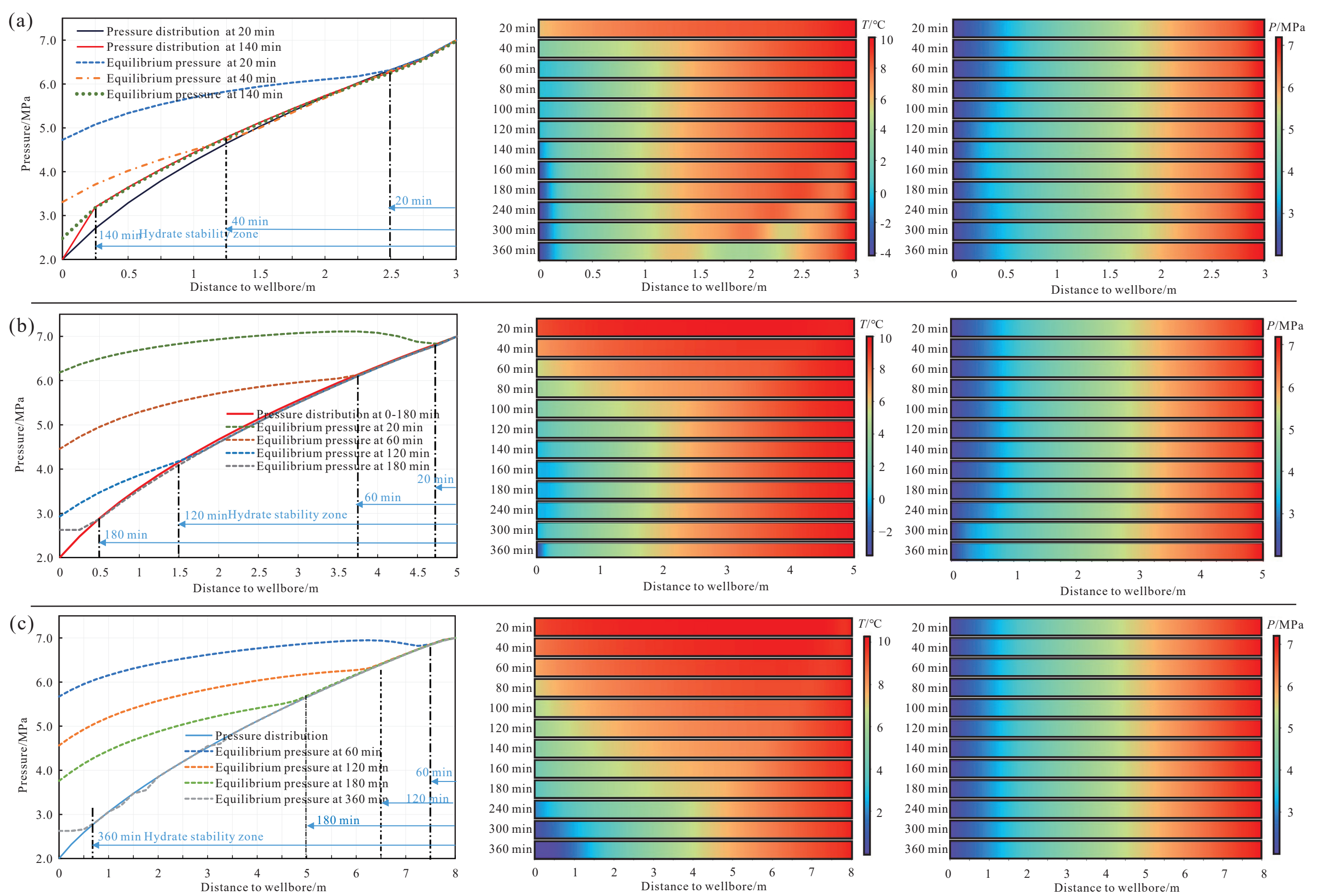

Fig. 11. Distribution of reservoir pressure and equilibrium pressure of hydrates over time when the dissociation front is (a) 3 m, (b) 5 m, (c) 8 m away from the production well, as well as distribution of reservoir temperature and pressure in the hydrate dissociation zone.

4. Multiphase seepage mechanism in NGHs dissociation zone

4.1. Isothermal adsorption characteristics of methane in NGHs dissociation zone

The seepage of multi-phase flow such as the gas and water from hydrate dissociation mainly occurs in the area between the production well shaft and the NGHs dissociation front. Given the high clay mineral content and the high proportion of micro/nanopores in NGHs reservoirs in the SCS, the authors carried out the methane isothermal adsorption experiments of the dissociation zone, obtaining the following results. Under dry condition, clayey silt reservoirs had a methane adsorption capacity equivalent to that of shale when their temperature was lower than that of shale (Fig. 13a). Moreover, the methane adsorption capacity was close to that of illites, slightly lower than that of kaolinites and chlorites, and far lower than that of montmorillonites under dry condition (Fig. 13b). Under the same temperature, the methane adsorption curves generally rose with an increase in pressure until the press reached a certain value, at which some adsorption curves started to rise slowly or drop (Fig. 13c). Under moist conditions, the water content hardly affected, decreased, and increased the methane adsorption capacity, respectively when the pressure was below 2 MPa, 2–10 MPa, and above 10 MPa (Fig. 13d). The experimental data revealed that the modified Langmuir model can well reflect the methane isothermal adsorption at low pressure, while the Dubinin-Radushevich equation can be used to characterize the methane isothermal adsorption at medium-high pressure (Fig. 14; Qi RR et al., 2022).

The above experiment discovered that clayey silt reservoirs in the SCS have the adsorption of methane for the first time. This adsorption of methane has important effects on the gas-water two-phase seepage in the NGHs dissociation zone. This discovery will guide the in-depth research on NGHs exploitation mechanism, the establishment of the decoupling method for production capacity simulation, and selecting reservoir stimulation methods.

4.2. Changes in the microscopic pore structure and permeability of reservoirs in hydrate dissociation zone

As shown by the NGHs production tests in the SCS, different depressurization methods will lead to a surge in the rate of pressure decrease around the production well shaft. Moreover, the fluid migration around the production well will cause fine sediment particles to accumulate at and plug the parts where pores narrow, leading to a substantial decrease in the absolute permeability of reservoirs. Based on the CT and digital core technologies, the authors researched the sensitivity of flow rate in porous media in clayey silts under different displacement pressures for the first time using the CT technology-based device form measuring the changes in the clayey silt reservoirs in sea areas (Qin XW et al., 2019). This research allowed for obtaining the critical pressure at which pores and throat structures of clayey silt reservoirs deform and revealing the main controlling factors in the decrease in the absolute permeability of reservoirs.

The permeability of porous media in clayey silts decreases with an increase in displacement pressure, and 3 MPa/m is the critical pressure gradient for the sharp change in the pore structure and permeability of clayey silt reservoirs. Specifically, the pore structure will creep but the pore structure and permeability will both remain relatively stable when the pressure gradient is less than 3 MPa/m. The pore structure will be rapidly destroyed when the pressure gradient is more than 3 MPa/m, resulting in irreversible reduction in the permeability (Figs. 15a, b). In essence, the permeability is reduced by external forces. Specifically, the pore space deforms with an increase in the displacement pressure, causing the distribution of pores and throats allowing for fluid seepage to narrow in general. As a result, the number of small throats increases, the number of large throats decreases, the average and median pore throat radii decrease, and the maximum pore throat radius decreases (Figs. 15c, d; Cai JC et al., 2020).

4.3. Gas-water two-phase seepage capacities of clayey silts in dissociation zone

The gas-water two-phase relative permeability curves can effectively reflect the dynamic seepage characteristics of one phase in reservoirs in the case of the co-existence of gas and water from hydrate dissociation. Using the simulation system for the radial flow in geological reservoirs, the authors researched the evolutionary laws of gas-water two-phase seepage capacities in clayey silt reservoirs in the hydrate dissociation zone under different overburden pressures for the

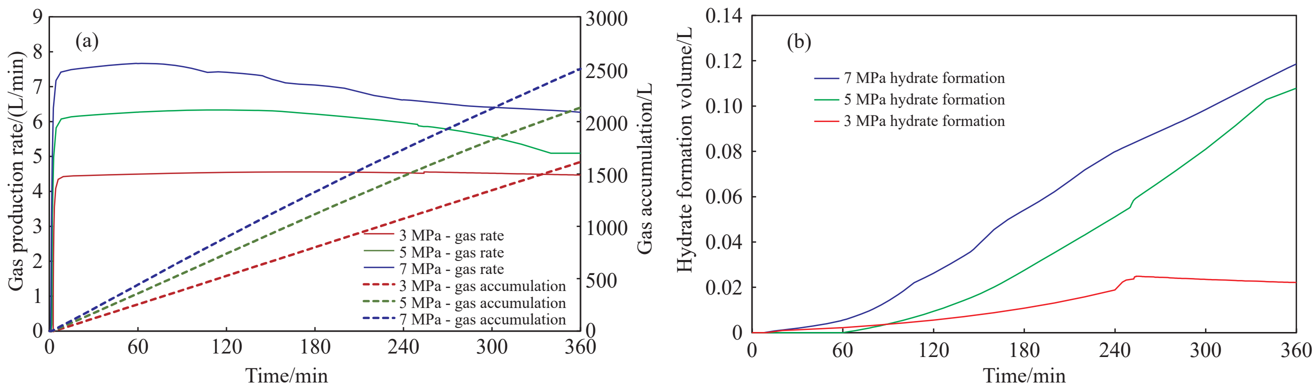

Fig. 12. Production curves of gas production rate (a) and secondary hydrate formation (b) under different pressure differences.

first time. As a result, they obtained the gas-water two-phase relative permeability curves and preliminarily determined the dynamic changes in the complex multi-phase and multi-field seepage capacities around production wells.

Owing to the high clay mineral content, gas is difficult to enter small throats to achieve effective gas displacement in the process of two-phase seepage in clayey silts. The increase in gas saturation leads to severe interference between gas and water, which affects the fluidity of gas phase. As a result, the maximum effective relative permeability of gas is less than 0.1, reflecting that the gas-water two-phase flow produced from hydrate dissociation in clayey silts are difficult to be discharged from the hydrate dissociation zone. Moreover, as revealed by the two-phase relative permeability curves of clayey silt reservoirs, the isotonic points shift more to the right and has a lower location, the two-phase flow area is narrower, and the maximum gas relative permeability is lower compared to those of other types of reservoirs such as sandstone reservoirs. These characteristics indicate a lower flow capacity of gas in clayey silt reservoirs. Therefore, to further increase the gas production, it is necessary to conduct effective reservoir stimulation (Fig. 16). Moreover, it is necessary to further conduct in-depth research on the multiphase seepage law under the complex conditions such as the creepage deformation of reservoir structure and the continuous changes in absolute permeability caused by large NGHs production-induced pressure difference.

5. Optimization of reservoir seepage capacity and regulation of hydrate gas production

5.1. Seepage capacity optimization and temperature field reformation of reservoirs

The seepage capacity of reservoirs is a key factor affecting the long-term, stable, and efficient hydrate exploitation. During hydrate exploitation, the hydrate dissociation in clayey silts will affect the effectiveness of proppants artificially injected into the original reservoir stimulation area around a production well, making it difficult to maintain the high conductivity of reservoirs around the well for a long time. Owing to the increased risks of the closure and failure of the reservoir stimulation area, the permeability enhancement effect achieved by initial stimulation will be undermined as the hydrate exploitation goes on. Meanwhile, the temperature

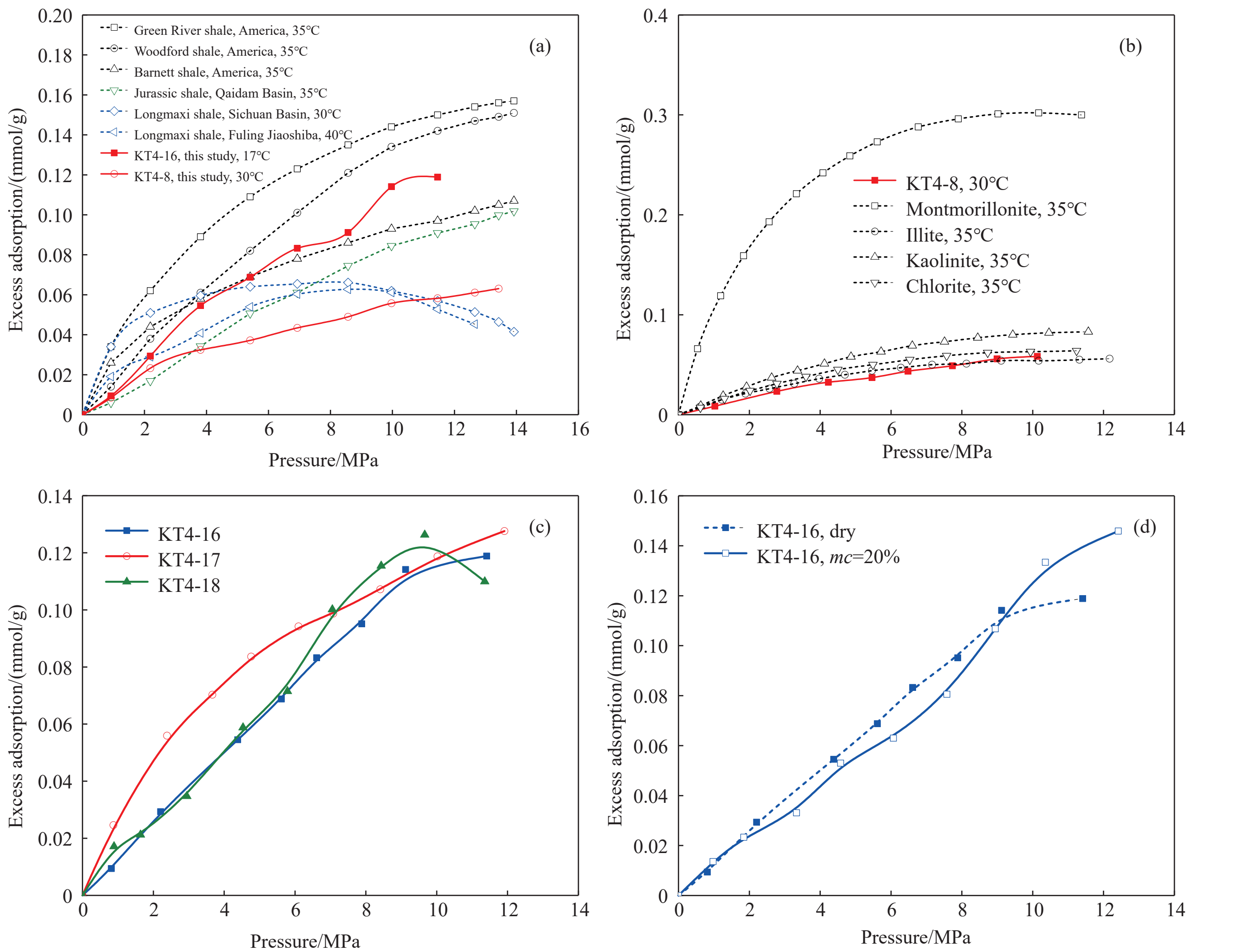

Fig. 13. a–Comparison of the methane adsorption capacities of shale, clayey silts, and coal under different pressures; b–comparison of the adsorption capacities of clay minerals and clayey silts under different pressure; c–methane isothermal adsorption curves of clayey silt samples under dry condition; d–comparison of isothermal adsorption curves of clayey silts under dry and moist conditions (after Qi RR et al., 2022).

of the stimulation area decreases with the continuous exploitation of hydrates, causing secondary hydrates or ice to form, which gradually occupy sediment pores and plug their throats, thus leading to the further increase in the risks of gas production reduction. Therefore, compared with initial reservoir stimulation, secondary reservoir stimulation is more important for long-term hydrate exploitation and continuous permeability enhancement. Previous studies of reservoir seepage capacity mainly focus on initial reservoir stimulation and optimization (Chaouachi M et al., 2015; Cao QY et al., 2017; Too JL et al., 2018; Chen Q et al., 2020; Luo TY et al., 2020; Yao YX et al., 2020; Yang L et al., 2020), while the influencing mechanisms of secondary reservoir stimulation on permeability enhancement and production increase are not yet studied.

Regarding the suitability evaluation and fracture propagation mechanisms of secondary reservoir stimulation, the authors conducted hydraulic fracturing and CT imaging experiments on hydrate reservoir samples collected from the SCS using the independently developed device for fracturing experiments clayey silt reservoirs (Qin XW et al., 2019). The experiment results show that fine-grained sediments in the hydrate dissociation zone are prone to form fractures and thus secondary stimulation is applicable. The clay minerals in the clayey silt reservoirs swell in contact with water, greatly enhancing the plasticity of the reservoirs. Consequently, more energy in strata will be consumed to propagate fractures. With an increase in the confining pressure, the plastic deformation degree of clayey silts increases, relatively simple horizontal fractures and small fracture zones are more prone to form, and the fracture constantly widen. As the pumping pressure continuous increases, large amounts of micro-fractures are prone to occur around boreholes (Fig. 17). Regarding the temperature field reformation and regulation mechanism, the authors proposed an innovative method for hydrate exploitation by depressurization and backfilling with in-situ supplemental heat. In this method, CaO powder is injected into hydrate-bearing layers, and the exothermic reactions between CaO and water from hydrate dissociation could provide abundant in situ heat to supplement the formation heat consumed by hydrate dissociation. Moreover, the authors put forward the hydrate exploitation scheme, key technologies, and technical process of the new method. The numerical simulation shows that this new technology

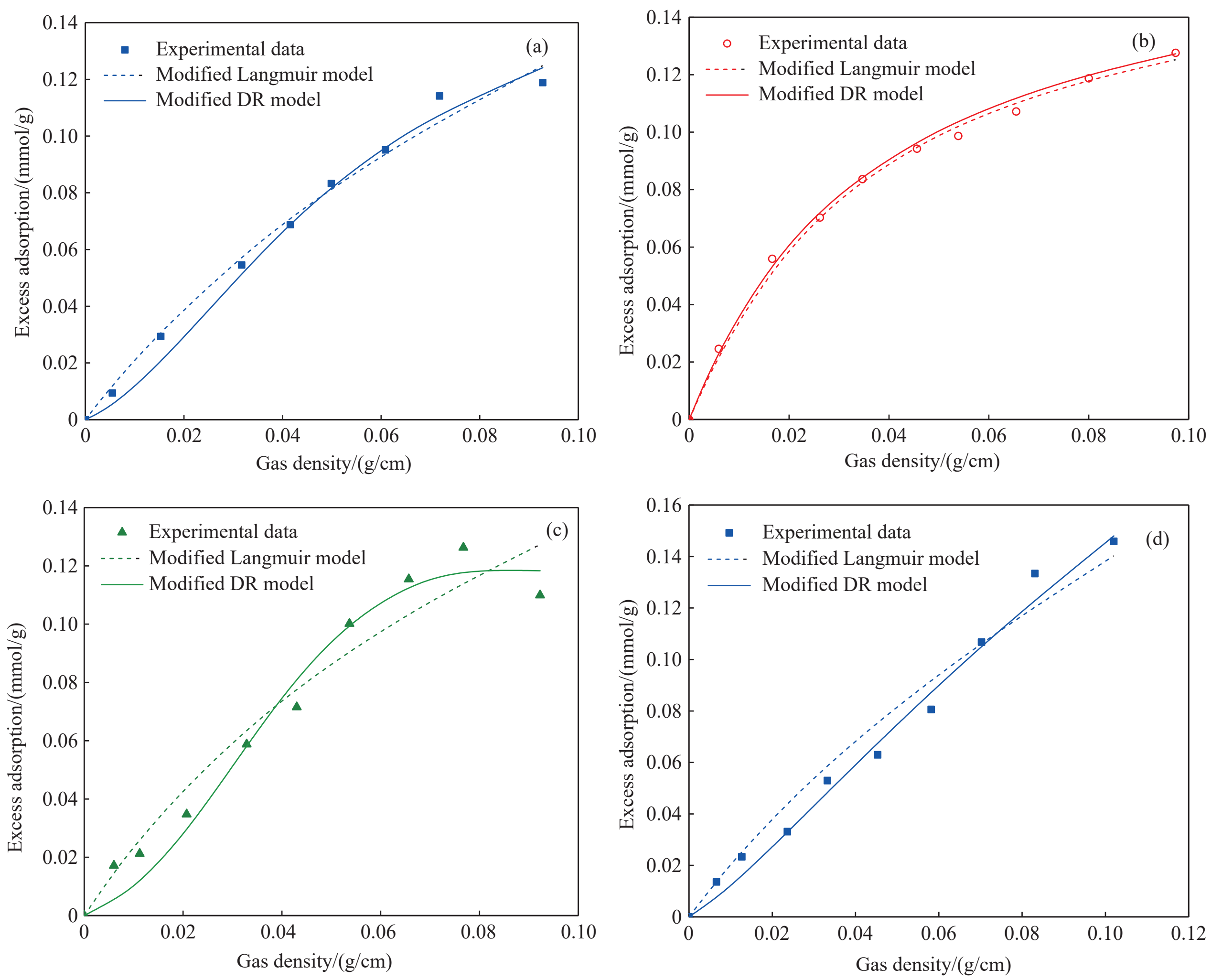

Fig. 14. Simulation results of samples (a) KT4-16 (dry condition), (b) KT4-17 (dry condition), (c) KT4-18 (dry condition), and (d) KT4-16 (moist condition) using the modified Langmuir and DR models (after Qi RR et al., 2022).

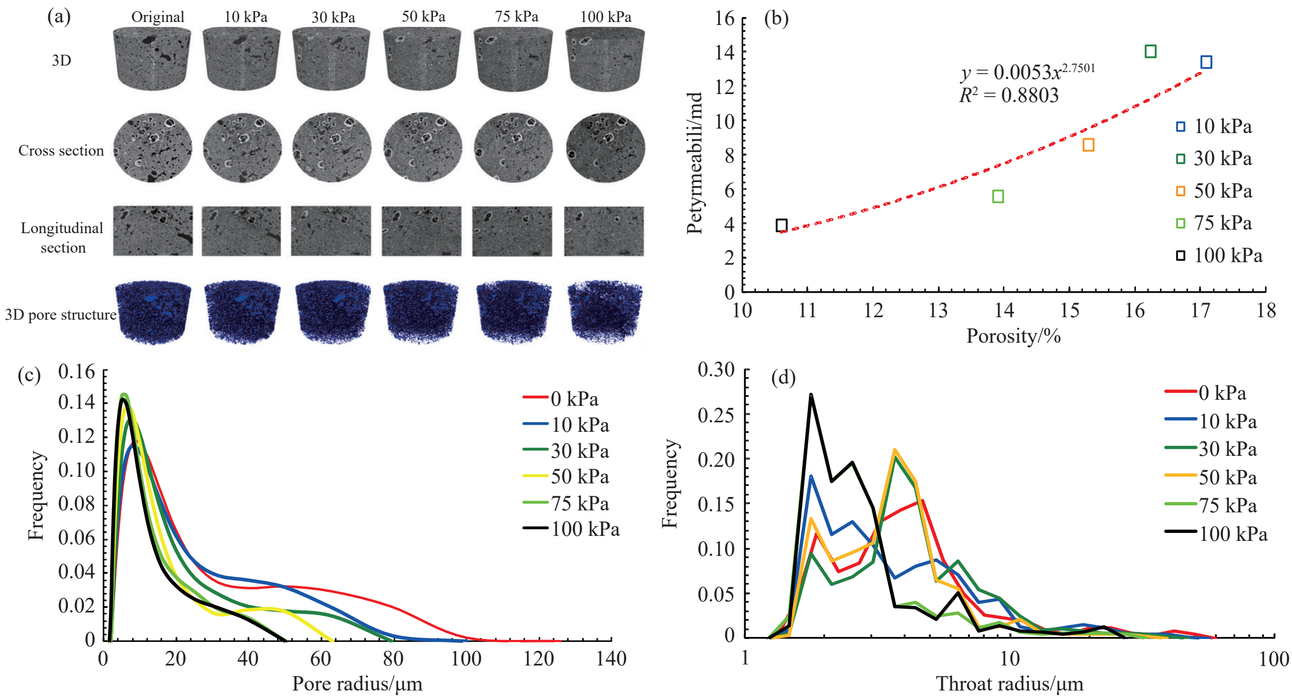

Fig. 15. The three-dimensional, cross-sectional, and longitudinal sections and pore reconstruction CT images of the fourth experimental sample under different pressures. a–the pixel resolution of the sample was about 3 μm; b–porosity versus permeability for the fourth set experiments; c–pore size distribution of the clayey-silt sample under different axial stresses; d–throat size distribution of the clayey-silt sample under different axial stresses (after Cai JC et al., 2020).

combined with fracturing of horizontal wells can significantly increase gas production and that fracture permeability and CaO powder quantity are key parameters restricting the hydrate recovery in this method (Li SD et al., 2020). In future research, it is necessary to further determine the support and enhancement mechanisms of reservoir stimulation, define the method for actively regulating the seepage capacity, verify this method through large-scale physical simulation experiments, and conduct engineering feasibility assessment.

5.2. Simulation and regulation of gas production in hydrate exploitation

Numerical simulation is considered an important method for predicting the dynamics of hydrate exploitation and identifying sensitive factors in hydrate exploitation and also an important platform for regulating NGHs production capacity. Moreover, simulators serve as essential tools of numerical simulation. The presently common simulators mainly include TOUGH + Hydrate, TOUGH-Fx/Hydrate, MH21-HYDRES, FEHM, GPRS-HYDRATE, and CMG STARS (Lu HL et al., 2021). In combination with the characteristics of NGHs reservoirs in the SCS, the authors have developed the hydrate engine platform (Hydrate Smart V1.0; Qin XW, 2019), the comprehensive management platform of reservoir physical property data (GH Properties V1.0; Qin XW, 2021), and the onsite data analysis platform for hydrate production and tests (Hydrate Captain V1.0; Lu C, 2020). Compared with foreign simulators of the same types, Hydrate Smart V1.0 has the functions such as model definition, the processing of physical parameters and hydrate

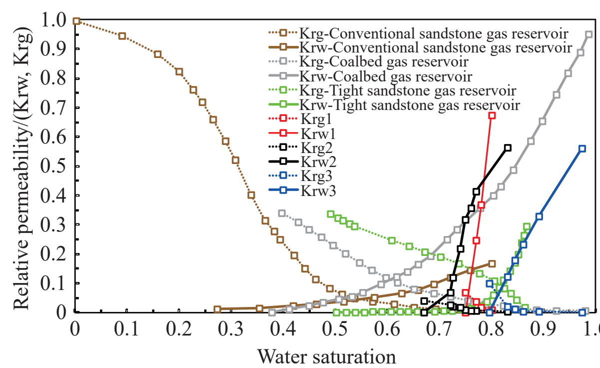

Fig. 16. Relative permeability curves of other gas reservoirs (after Lu C et al., 2021).

characteristics, well section models, production control, equilibrium initialization, and simulation calculation besides a series of functions for matrix model building, such as grid definition, structure models, attribute models, lithology zoning, and grid screening. Moreover, it can provide comprehensively judgement on the simulation results by applying one-dimensional curves, two-dimensional planes, two-dimensional sections, and three-dimensional views (Fig. 18). The authors carried out a simulation study of the first NGHs production test by a vertical well using the independently developed hydrate numerical simulators, obtaining the following simulation results. In the first 60 days of the first NGHs production test, the hydrate reservoirs featured a dissociation radius of about 5 m, and the gas production from hydrate dissociation accounted for approximately 85% of the accumulative gas production. If the

NGHs exploitation by depressurization in a vertical well continued, the conduction of the pressure drop funnel would be restricted, leading to a decrease in the gas production rate of hydrate dissociation. Furthermore, the temperature and pressure of hydrate reservoirs were not favorable for the formation of secondary hydrates in the first 60 days. However, large amounts of secondary hydrates would form at hydrate dissociation front in the long-term NGHs exploitation. These results provide important theoretical support for our innovative proposal to implement the second NGHs production test using horizontal wells (Fig. 19).

Depressurization strategy is an important basis for guiding production system preparation and regulating the production capacity in hydrate production tests. Based on the comprehensive research on the reservoir structure characterization, hydrate phase transition, two-phase seepage, reservoir seepage capacity, and the dynamic characteristics of the first production test in the SCS, the authors put forward a depressurization strategy for the hydrate exploitation in horizontal wells, that is, slowly reducing the bottomhole pressure to prevent the formation of ice and secondary hydrates, maintaining the effective seepage capacity of reservoirs for a long time, and steadily increasing the production pressure difference to increase the gas production. This depressurization strategy has been applied to and verified in the second NGHs production test in the SCS.

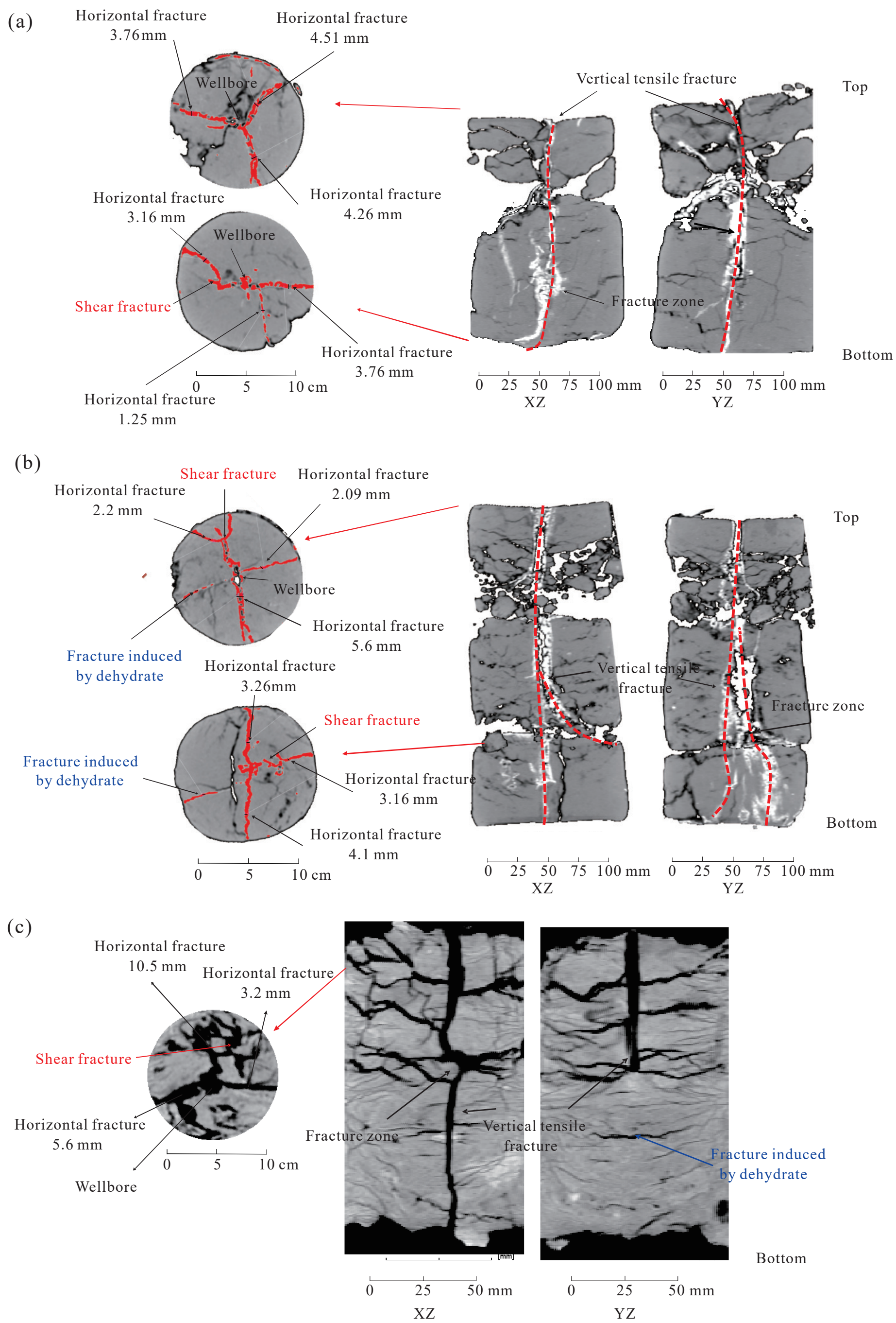

Fig. 17. Fracture characteristics of samples 1-3 after hydraulic fracturing by CT (after Lu C et al., 2021).

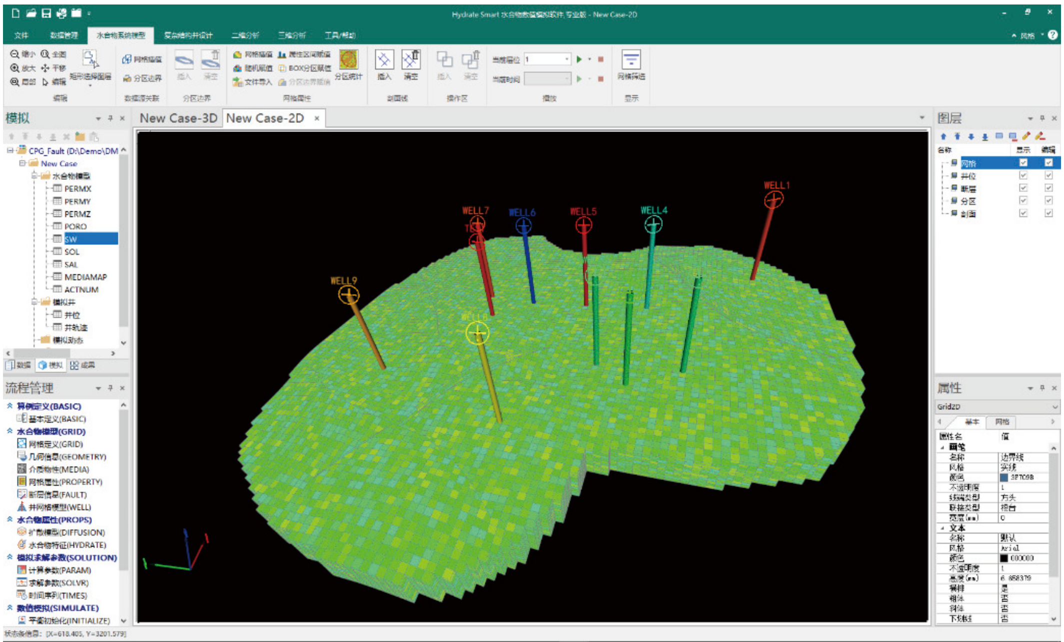

Fig. 18. Interface of hydrate smart platform (after Sun JS et al., 2021).

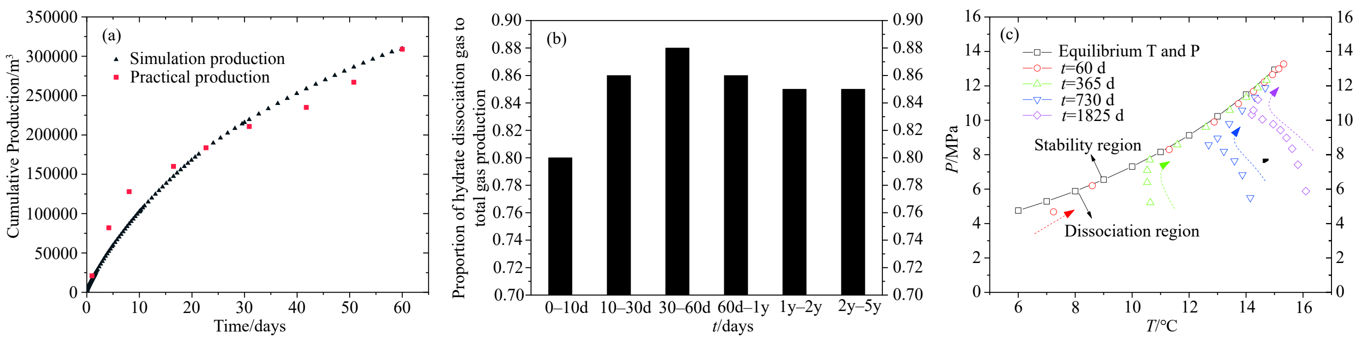

Fig. 19. a–Comparison between simulated and practical gas production during the first offshore NGHs production test. b–the proportion of gas from NGHs dissociation to total gas production in different stages of hydrate exploitation. c–comparative relationship between the temperature and pore pressure conditions of hydrate-bearing layers and the hydrate equilibrium condition in different stages of hydrate exploitation (after Qin XW et al., 2020).

6. Conclusions and recommendations for future research

The SCS enjoys enormous potential for the exploration and development of NGHs resources. As suggested by in-depth research on the two NGHs production tests in the Shenhu Area in the northern SCS, it is crucial to study the NGHs exploitation mechanisms, and key factors restricting the gas production efficiency of hydrate dissociation include reservoir structure characterization, hydrate phase transition, multiphase seepage and permeability enhancement, and the simulation and regulation of production capacity, among which the hydrate phase transition and seepage mechanism are crucial. Study results reveal that the hydrate phase transition in the SCS is featured by low dissociation temperature and is prone to produce secondary hydrates in reservoirs and that it is a complex process under the combined effects of the seepage, stress, temperature, and chemical fields. The multiphase seepage is mainly controlled by multiple factors such as the physical properties of unconsolidated reservoirs, hydrate phase transition, and exploitation method and is characterized by the strong adsorption of methane, the abrupt change in absolute permeability, and weak flow capacity of gas. Therefore, to ensure the long-term, stable, and efficient NGHs exploitation in the SCS, it is necessary to further enhance the reservoir seepage capacity and increase gas production through secondary reservoir stimulation based on initial reservoir stimulation.

With the constant progress in the NGHs industrialization, great efforts should be made to tackle the difficulties such as determining the micro-change in temperature and pressure, the response mechanisms of material-energy exchange, the methods for efficient NGHs dissociation, and the boundary conditions for the formation of secondary hydrates in the large-scale, long-term gas production in the perspective of basic theory of the NGHs exploitation in the SCS. The authors recommend carrying out research on the following aspects:

(i) Regarding physical properties of reservoirs: It is necessary to shift the focus from the porous media in clayey silts in the hydrate dissociation zone to the hydrate-bearing sediments at the hydrate dissociation front; to determine the effects of the microscopic distribution of hydrates at different states in the front area on basic physical property parameters such as the porosity and permeability by relying on the static, microscopic visualization technology; and to establish the mechanism of reservoir energy supply from the change in hydrate dissociation front during hydrate exploitation.

(ii) Regarding hydrate phase transition: It is necessary to enhance the research on the formation and dissociation dynamics of hydrate-bearing clayey silts and the crystallization dynamics and inhibition mechanism of secondary hydrates; and to improve the current water molecular force field models and solid molecular models used for molecular dynamics simulation to build a dynamic model closer to the actual sediment conditions in the SCS. Moreover, it is necessary to further improve the experimental simulation devices based on the core scale, to determine the method for characterizing physical property parameters of hydrate-bearing sediments at different hydrate occurrence states in the process of continuous phase transition; and to establish the mathematical model of the dynamic evolution of physical property parameters.

(iii) Regarding multi-phase seepage and permeability enhancement: It is necessary to obtain the parameters on the dynamic changes in the relative permeability and capillary pressure of hydrate-bearing reservoirs in the hydrate dissociation zone (i.e., from the production well shaft and the hydrate dissociation front) on a core scale; to clarify the law of multiphase seepage and its primary controlling factors; and to establish relative permeability models on scales from cores to the mining area. Furthermore, it is necessary to perform the research on the secondary stimulation, permeability enhancement, and production increase of hydrate reservoirs; to clarify the support and enhancement mechanisms for unconsolidated reservoir stimulation and the temperature field reformation mechanism; to develop new matching materials and techniques; to grasp the changes in reservoir seepage capacity under different control modes of phase transition; and to assess the effects of gas production increase achieved using different methods.

(iv) Regarding the regulation of production capacity: it is necessary to constantly iterate and update the numerical calculation models of hydrate phase transition, seepage, and coupling of various complex effects; to improve the accuracy of production capacity simulation; to clarify the main factors restricting the gas production efficiency of hydrates; and to establish the regulation mechanism of production capacity applicable to various production test scenarios.

CRediT authorship contribution statement

Xu-wen Qin conceived the presented idea. Xu-wen Qin, Cheng Lu and Ping-kang Wang prepared the manuscript. Qian-yong Liang designed the figures. All authors discussed the results and contributed to the final manuscript.

Declaration of competing interest

The authors declare no conflicts of interest.

Acknowledgement

This project is funded by a key project of the National Natural Science Foundation of China entitled “Multi-Field Spatio-Temporal Evolutionary Pattern of Hydrate Phase Transition and Seepage of NGHs Reservoirs” (51991365)

References

Bian H, Xia YX, Lu C, Qin XW, Meng QB. 2020. Pore structure fractal characterization and permeability simulation of natural gas hydrate reservoir based on CT images. Geofluids, 6934691. doi: 10.1155/2020/6934691.

Cai JC, Hu XY. 2015. Fractal Theory in Porous Media and Its Applications. Science Press (in Chinese).

Cai JC, Xia YX, Lu C, Bian H, Zou SG. 2020. Creeping microstructure and fractal permeability model of natural gas hydrate reservoir. Marine and Petroleum Geology, 115, 104282. doi: 10.1016/j.marpetgeo.2020.104282.

Cai JC, Xia YX, Xu S, Tian HT. 2020. Advances in multiphase seepage characteristics of natural gas hydrate sediments. Chinese Journal of Theoretical and Applied Mechanics, 52(1), 208–223. doi: 10.6052/0459-1879-19-362.

Cao YQ. 2017. Fracability of Reservoirs in Frozen Soil. Qingdao, China University of Petroleum (East China), Ph. D thesis, 21 –69 (in Chinese with English abstract).

Chaouachi M, Falenty A, Sell K. 2015. Microstructural evolution of gas hydrates in sedimentary matrices observed with synchrotron X-ray computed tomographic. Geochemistry, Geophysics, Geosystems, 16 (6), 1711–1722. doi: 10.1002/2015GC005811.

Chen L, Feng YC, Kogawa T. 2018. Construction and simulation of reservoir scale layered model for production and utilization of methane hydrate: The case of Nankai Trough Japan. Energy, 143, 128–140. doi: 10.1016/j.energy.2017.10.108.

Chen Q, Hu GW, Li YL, Wan YZ, Liu CL, Wu NY, Liu Y. 2020. A prospect review of new technology for development of marine gas hydrate resources. Marine Geology Frontiers, 36(9), 44–55. doi: 10.16028/j.1009-2722.2020.081.

Fan ZB, Sun CM, Kuang YM. 2017. MRI analysis for methane hydrate dissociation by depressurization and the concomitant ice generation. Energy Procedia, 105, 4763–4768. doi: 10.1016/j.egypro.2017.03.1038.

Gao DL. 2020. Discussin on development modes and engineering techniques for deepwater natural gas and its hydrates. Natural Gas Industry, 40(8), 136–143. doi: 10.3787/j.issn.1000-0976.2020.08.014.

Geng LT, Cai J, Lu C, Qin XW, Qi RR, Meng FL, Xie Y, Sha ZB, Wang XH, Sun CY. 2021. Phase equilibria of natural gas hydrates in bulk brine and marine sediments from the South China Sea. Journal of Chemical and Engineering Data, 66, 4064–4074. doi: 10.1021/acs.jced.1c00307.

Hauge LP, Birkedal KA, Ersland G, Graue A. 2014. Methane production from natural gas hydrates by CO_2 replacement-review of lab experiments and field trial. Proceedings of the SPE Bergen One Day Seminar, SPE–169198-MS. doi: 10.2118/169198-MS.

Heeschen KU, Schicks JM, Oeltzschner G. 2016. The promoting effect of natural sand on methane hydrate formation: Grain sizes and mineral composition. Fuel, 181, 139–147. doi: 10.1016/j.fuel.2016.04.017.

Khurana M, Yin Z, Linga P. 2017. A review of clathrate hydrate nucleation. ACS Sustainable Chemistry and Engineering, 5(12), 11176–11203. doi: 10.1021/acssuschemeng.7b03238.

Kondori J, Zendehboudi S, Hossain ME. 2017. A review on simulation of methane production from gas hydrate reservoirs: Molecular dynamics prospective. Journal of Petroleum Science and Engineering, 159, 754–772. doi: 10.1016/j.petrol.2017.09.073.

Kumar SawV, Udayabhanu G, Mandal A, Laik S. 2015. Methane Hydrate Formation and Dissociation in the Presence of Silica Sand and Bentonite Clay. Oil Gas Sci. Technol., 70, 1087–1099. doi: 10.2516/ogst/2013200.

Lei X, Yao YB, Qin XW, Lu C, Luo WJ, Wen ZA, Yuan XH. 2022. Pore structure changes induced by hydrate dissociation: An example of the unconsolidated clayey-silty hydrate bearing sediment reservoir in the South China Sea. Marine Geology, 443, 106689. doi: 10.1016/j.margeo.2021.106689.

Li JF, Ye JL, Qin XW, Qiu HJ, Wu NY, Lu HL, Xie WW, Lu JA, Peng F, Xu ZQ, Lu C, Kuang ZG, Wei JG, Liang QY, Lu HF, Kou BB. 2018. The first offshore natural gas hydrate production test in South China Sea. China Geology, 1, 5–16. doi: 10.31035/cg2018003.

Li SD, Li X, Wang SJ, Sun YM. 2020. A novel method for natural gas hydrate production: depressurization and backfilling with in-situ supple-mental heat. Journal of Engineering Geology, 28(2), 282–293. doi: 10.13544/j.cnki.jeg.2020-061.

Li SX, Guo SP, Chen MY, Zhang NT, Wu DD. 2020. Advances and recommendations for multi-field characteristics and coupling seepage in natural gas hydrate development. Chinese Journal of Theoretical and Applied Mechanics, 2020,52(3), 828–842. doi: 10.6052/0459-1879-20-050.

Li SX, Wang ZQ, Li S. 2021. Investigations on performance of hydrate dissociation by depressurization near the quadruple point. Journal of Natural Gas Science and Engineering, 90, 1–12. doi: 10.1016/j.jngse.2021.103929.

Li XS. 2008. Progress in researches on exploration and exploitation for natural gas hydrate. Modern Chemical Industry, 28(6), 1–15. doi: 10.16606/j.cnki.issn0253-4320.2008.06.019.

Li Z, Tian X, Li Z, Xu J, Zhang H, Wang D. 2020. Experimental study on growth characteristics of pore-scale methane hydrate. Energy Reports, 6, 933–943. doi: 10.1016/j.egyr.2020.04.017.

Liu W, Cui S, Wang Z, Ding B. 2019. Research progress on adsorbent materials for gas hydrate exploitation by displacement method. Modern Chemical Industry, 11, 53–57. doi: 10.16606/j.cnki.issn0253-4320.2019.11.012.

Liu W, Wang S, Yang M, Song Y, Wang S, Zhao J. 2015. Investigation of the induction time for THF hydrate formation in porous media. Journal of Natural Gas Science and Engineering, 24, 357–364. doi: 10.1016/j.jngse.2015.03.030.

Lu C, Ma C, Geng LT, Yu L, Bian H, Qi RR, Xing DH, Mao WJ, Meng FL. 2021. Device for simulating the formation and evolution of NGH inverse phase transition. 2021.08. 17, China, ZL202023152284.6.

Lu C, Qin XW, Ma C, Bian H, Cui YD, Rao Y. 2020. Onsite data analysis platform for hydrate production and tests—Hydrate Captain V1. 0. 2020. 01. 3, 2020SR0916459.

Lu C, Qin XW, Mao WJ, Ma C, Geng LT, Yu L, Bian H, Meng F, Qi RR. 2021. Experimental study on the propagation characteristics of hydraulic fracture in clayey-silt sediments. Geofluids, 6698649. doi: 10.1155/2021/6698649.

Lu C, Qin XW, Yu L, Geng LT, Mao WG, Bian H, Meng F. 2021. The characteristics of gas-water two-phase radial flow in clay-silt sediment and effects on hydrate production, Geofluids, 6623802. doi: 10.1155/2021/6623802.

Lu C, Sun XX, Li ZZ, Ma C, Wang JL, Geng LT, Zhang Kw. 2019. Simulation system for the radial flow in geological reservoirs. 2019.09. 17, China, ZL201821818171.5.

Lu C, Xia YX, Sun XX, Bian H, Qiu HJ, Lu HF, Luo WJ, Cai JC. 2019. Permeability evolution at various pressure gradients in natural gas hydrate reservoir at the Shenhu Area in the South China Sea. Energies, 12(19), 3688. doi: 10.3390/en12193688.

Lu H, Matsumoto R. 2002. Preliminary experimental results of the stable P-T conditions of methane hydrate in a nannofossil-rich claystone column. Geochemical Journal, 36(1), 21–30. doi: 10.2343/geochemj.36.21.

Lu HL, Shang SL, Cheng XJ, Qin XW, Gu LJ, Qiu HJ. 2021. Research progress and development direction of numerical simulator for natural gas hydrate development. Acta Petrolei Sinica, 42(11), 1516–1530. doi: 10.7623/syxb202111011.

Luo TY, Feng Y, Hu RD, Shi YH. 2020. Fracturing technology of subsea gas hydrate reservoir. Drilling & Production Technology, 43(4), 67–70.

Lü Q, Zang, XR, Li XS, Li G. 2018. Effect of seawater ions on cyclopentane-methane hydrate phase equilibrium. Fluid Phase Equilibria, 458, 272–277. doi: 10.1016/j.fluid.2017.11.031.

Moridis GJ, Collett TS, Dallimore S, Inoue T, Mroz T. 2005. Analysis and interpretation of the thermal test of gas hydrate dissociation in the JAPEX/JNOC/GSC et al. Mallik 5L-38 gas hydrate production research well. Bulletin-Geological Survey of Canada.

Mu L, Cui QY. 2019. Experimental study on the dissociation equilibrium of (CH4 + CO2 + N2) hydrates in the mixed sediments. Journal of Chemical and Engineering Data, 64(12), 5806–5813. doi: 10.1021/acs.jced.9b00760.

Ning FL, Liang JQ, Wu NY, Zhu YH, Wu SG, Liu CL, Wei CF, Wang DD, Zhang H, Xu M, Liu ZC, Li J, Sun JX, Ou WJ. 2020. Reservoir characteristics of natural gas hydrates in China. Natural Gas Industry, 40(8), 1–24. doi: 10.3787/j.issn.1000-0976.2020.08.001.

Numasawa M. 2008. Objectives and operation over view of the JOGMEC/NRCan /Aurora Mallik gas hydrate production test. Proceedings of the 6th International Conference on Gas Hydrates.

Oyama A, Masutani SM. 2017. A review of the methane hydrate program in Japan. Energies, 10(10), 1447. doi: 10.3390/en10101447.

Qi RG, Qin XW, Bian H, Lu C, Yu L, Ma C. 2021. Overview of molecular dynamics simulation of natural gas hydrate at nanoscale. Geofluids, 6689254. doi: 10.1155/2021/6689254.

Qi RR, Qin XW, Lu C, Ma C, Mao WJ, Zhang WT. 2022. Experimental study on the isothermal adsorption of methane gas in natural gas hydrate argillaceous silt reservoir. Advances in Geo-Energy Research, 6(2), 143–156. doi: 10.46690/ager.2022.02.06.

Qin XW, Liang QY, Ye JL, Yang L, Qiu HJ, Xie WW, Liang JQ, Lu JA, Lu C, Lu HL, Ma BJ, Kuang ZG, Wei JG, Lu Hf, Kou BB. 2020. The response of temperature and pressure of hydrate reservoirs in the first gas hydrate production test in South China Sea. Applied Energy, 278, 115649. doi: 10.1016/j.apenergy.2020.115649.

Qin XW, Lu C, Ma C. 2019. Hydrate engine platform—Hydrate Smart V1. 0. 2019. 11. 01, 2019sr1329033.

Qin XW, Lu C, Tian YY, Bian H, Meng FL, Cui YD. 2021. Comprehensive management platform of reservoir physical property data—GH Properties V1. 0. 2021. 02. 10, 2021SR0245278.

Qin XW, Lu JA, Lu HL, Qiu HJ, Liang JQ, Kang DJ, Zhan LS, Lu HF, Kuang ZG. 2020. Coexistence of natural gas hydrate, free gas and water in the gas hydrate system in the Shenhu Area, South China Sea. China Geology, 3(2), 210–220. doi: 10.31035/cg2020038.

Qin XW, Ye JL, Qiu HJ, Lu C, Sun XX, Ma C, Li ZZ, Wan TH. Geng LT, Zhang X, Zhang KW. 2019. CT technology-based device form measuring the changes in the clayey silt reservoirs in sea areas. 2019.07. 16, China, ZL201821815838.6.

Qin XW, Ye JL, Qiu HJ, Zhang JH, Lu C, Ma C, Li ZZ, Wan TH, Geng LT, Sa RN. 2019. Device for fracturing experiments of clayey silt reservoir. 2019.03. 15, China, ZL201821179508.2.

Qin Y, Pan Z, Liu Z. 2021. Influence of the particle size of porous media on the formation of natural gas hydrate: A review. Energy & Fuels, 35(15), 11640–11664. doi: 10.1021/acs.energyfuels.1c00936.

Schoderbek D, Farrell H, Howard J, Raterman K, Silpngarmlert S, Martin K, Smith B, Klein P. 2013. ConocoPhillips gas hydrate production test. United States. doi: 10.2172/1123878.

Sloan ED, Koh CA. 2007. Clathrate Hydrates of Natural Gases. New York, CRC press. doi: 10.1201/9781420008494.

Song GC, Li YX, Sum AK. 2020. Characterization of the Coupling between Gas Hydrate Formation and Multiphase Flow Conditions. Journal of Natural Gas Science and Engineering, 83, 103567. doi: 10.1016/j.jngse.2020.103567.

Su PB, Liang JQ, Zhang W, Liu F, Wang FF. 2020. Natural gas hydrate accumulation system in the Shenhu sea area of the northern South China Sea. Natural Gas Industry, 40(8), 77–89. doi: 10.3787/j.issn.1000-0976.2020.08.006.

Sun JS, Cheng YF, Qin XW, Sun YH, Jin Y, Wang ZY, Li SX, Lu C, Qu YZ, Lü KH, Wang CW, Wang JT, Wang R. 2021. The exploration and production test of gas hydrate and its research progress and exploration prospect in the northern South China Sea. Bulletin of National Natural Science Foundation of China, 35(6), 940–951.

Sun SC, Kong YY, Zhang Y, Liu CL. 2015. Phase equilibrium of methane hydrate in silica sand containing chloride salt solution. The Journal of Chemical Thermodynamics 90, 116–121. doi: 10.1016/j.jct.2015.06.030.

Teixeira AMA, Arinelli LDO, Medeiros JLD, Araújo O. 2018. Recovery of thermodynamic hydrate inhibitors methanol, ethanol and MEG with supersonic separators in offshore natural gas processing. Journal of Natural Gas Science and Engineering, 52, 166–186. doi: 10.1016/j.jngse.2018.01.038.

Terao Y, Lay K, Yamamoto K. 2014. Design of the surface flow test system for 1st offshore production test of methane hydrate. Offshore Technology Conference-Asia. doi: 10.4043/24719-MS.

Too JL, Cheng A, Linga P. 2018. Fracturing methane hydrate in sand: A review of the current status// Society of Petroleum Engineers Offshore. Kuala Lumpur, Malaysia, 28292. doi: 10.4043/28292-MS.

Uchida T, Takeya S, Chuvilin EM, Ohmura R, Nagao J, Yakushev VS, Istomin VA, Minagawa H, Ebinuma T, Narita H. 2004. Decomposition of methane hydrates in sand, sandstone, clays and glass beads. Journal of Geophysical Research:Solid Earth, 109(5), 1–12. doi: 10.1029/2003JB002771.

Wang P, Yang M, Chen B, Zhao Y, Zhao J, Song Y. 2017. Methane hydrate reformation in porous media with methane migration. Chemical Engineering Science, 168, 344–51. doi: 10.1016/j.ces.2017.04.036.

Wang PK, Zhu YH, Lu ZQ, Bai MG, Huang X, Pang SJ, Zhang S, Liu H, Xiao R. 2019. Research progress of gas hydrates in the Qilian Mountain permafrost, Qinghai, Northwest China: Review. SCIENTIA SINICA Physica, Mechanica and Astronomica, 49 (3), 034606. doi: 10.1360/SSPMA2018-00133.

Wei CF, Yan RT, Tian HH, Zhou JZ, Li WT, Ma TT, Chen P. 2020. Geotechnical status and challenges of natural gas hydrate exploitation. Natural Gas Industry, 40(8), 116–132. doi: 10.3787/j.issn.1000-0976.2020.08.009.

Wei N, Zhou SW, Cui ZJ, Zhao JZ, Zhang LH, Zhao J. 2020. Evaluation of physical parameters and construction of a parameter classification system for natural gas hydrate in the northern South China Sea. Natural Gas Industry, 40(8), 59–67. doi: 10.3787/j.issn.1000-0976.2020.08.004.

Wu NY, Huang L, Hu GW, Li YL, Cheng Q, Liu CL. 2017. Geological controlling factors and scientific challenges for offshore gas hydrate exploration. Marine Geology and Quaternary Geology, 37(5), 1–11. doi: 10.16562/j.cnki.0256-1492.2017.05.001.

Wu NY, Li YL, Liu LL, Wan YZ, Zhang ZC, Chen MT. 2021. Controlling factors and research prospect on creeping behaviors of marine natural gas hydrate-bearing-strata. Marine Geology and Quaternary Geology, 41(5), 3–11. doi: 10.16562/j.cnki.0256-1492.2021092201.

Wu NY, Li YL, Wan YZ, Sun JY, Huang L, Mao PX. 2020. Prospect of marine natural gas hydrate stimulation theory and technology system. Natural Gas Industry, 40(8), 100–115. doi: 10.3787/j.issn.1000-0976.2020.08.008.

Xu T, Zhang ZB, Li SD, Li X, Lu C. 2021. Numerical Evaluation of Gas Hydrate Production Performance of the Depressurization and Backfilling with an In Situ Supplemental Heat Method. ACS Omega, 6(18), 12274–12286. doi: 10.1021/acsomega.1c01143.

Yamamoto K, Kanno T, Wang XX. 2017. Thermal responses of a gas hydrate-bearing sediment to a depressurization operation. RSC Advance, 7(10), 5554–5577. doi: 10.1039/C6RA26487E.

Yang CZ, Luo KW, Liang JQ, Lin ZX, Zhang BD, Liu F, Su M, Fang YX. 2020. Control effect of shallow-burial deepwater deposits on natural gas hydrate accumulation in the Shenhu sea area of the northern South China Sea. Natural Gas Industry, 40(8), 68–76. doi: 10.3787/j.issn.1000-0976.2020.08.005.

Yang L, Shi FK, Zhang XH, Lu XB. 2020. Experimental studies on the propagation characteristics of hydrate fracture in clay hydrate sediment. Chinese Journal of Theoretical and Applied Mechanics, 52(1), 224–234. doi: 10.6052/0459-1879-19-179.

Yang L, Ye JL, Qin XW. 2021. Effects of the seepage capability of overlying and underlying strata of marine hydrate system on depressurization-induced hydrate production behaviors by horizontal well. Marine and Petroleum Geology, 128, 105019. doi: 10.1016/j.marpetgeo.2021.105019.

Yao YX, Li DL, Liang DQ. 2020. Research progress on hydraulic fracturing of natural gas hydrate reservoir. Advances in New and Renewable Enengy, 8(4), 282–290. doi: 10.3969/j.issn.2095-560X.2020.04.005.

Ye JL, Qin XW, Xie WW, Lu HL, Ma BJ, Qiu HJ, Liang GQ, Lu GA, Kuang ZG, Lu C, Liang QY, Wei SP, Yu YJ, Liu CH, Li B, Shen KX, Shi HX, Lu QP, Li J, Kou BB, Song G, Li B, Zhang HE, Lu HF, Ma C, Dong YF, Bian H. 2020. The second natural gas hydrate production test in the South China Sea. China Geology, 3(2), 197–209. doi: 10.31035/cg2020043.

Yu L, Zhang L, Zhang R. 2018. Assessment of natural gas production from hydrate-bearing sediments with unconsolidated argillaceous siltstones via a controlled sandout method. Energy, 160, 654–667. doi: 10.1016/j.energy.2018.07.050.

Yu M, Li W, Jiang L. 2017. Numerical study of gas production from methane hydrate deposits by depressurization at 274K. Applied Energy, 227, 28–37. doi: 10.1016/j.apenergy.2017.10.013.

Zhang L, Sun M, Sun L. 2019. In-situ observation for natural gas hydrate in porous medium: Water performance and formation characteristic. Magnetic Resonance Imaging, 65, 166–174. doi: 10.1016/j.mri.2019.09.002.

Zhang W, Liang JQ, Lu JA, Meng MM, He YL, Deng W, Feng JX. 2020. Characteristics and controlling mechanism of typical leakage gas hydrate reservoir forming system in the Qiongdongnan Basin, northern South China Sea. Natural Gas Industry, 40(8), 90–99. doi: 10.3787/j.issn.1000-0976.2020.08.007.

Zhang Y, Li XS, Wang Y, Chen ZY, Yan KF. 2016. Decomposition conditions of methane hydrate in marine sediments from South China Sea. Fluid Phase Equilibria, 413, 110–115. doi: 10.1016/j.fluid.2015.12.004.

Zhong GF, Zhang D, Zhao LX. 2020. Current states of well-logging evaluation of deep-sea gas hydrate-bearing sediments by international scientific ocean drilling (DSDP/ODP/IODP) programs. Natural Gas Industry, 40(8), 25–44. doi: 10.3787/j.issn.1000-0976.2020.08.002.

Zou CN, Tao SZ, Hou LH. 2013. Unconventional Petroleum Geology, 2nd Edition. Beijing, Geology Press, 1–258.